Microchemical Journal 144 (2019) 229–241

Contents lists available at ScienceDirect

Microchemical Journal

journal homepage: www.elsevier.com/locate/microc

Discrimination of Acacia gums by MALDI-TOF MS: applications to micro-samples from works of art☆

Clara Granzotto[a,b,*], Ken Sutherland[c], Julie Arslanoglu[a], Glen A. Ferguson[d]

[a] The Metropolitan Museum of Art, Scientific Research Department, 1000 5th Ave, New York, NY 10028, USA
[b] Northwestern University/Art Institute of Chicago Center for Scientific Studies in the Arts (NU-ACCESS), 2145 Sheridan Road, Evanston, IL 60208, USA
[c] The Art Institute of Chicago, Conservation Department, 111 South Michigan Ave, Chicago, IL 60603, USA
[d] Freelance Data Scientist, New York, USA

ARTICLE INFO

Keywords:
Plant gum
Acacia species
MALDI-TOF MS
Mass fingerprint
Binding media
Agglomerative clustering

ABSTRACT

This paper reports the discrimination of Acacia gums from the two most widely used and commercially significant species, *A. senegal* and *A. seyal*, using an innovative strategy based on matrix assisted laser desorption ionization-time-of-flight mass spectrometry (MALDI-TOF MS) after enzymatic digestion of the polysaccharide component. MALDI-TOF MS/MS experiments were carried out to determine the composition of the most intense ions of *A. seyal* gum and elucidate its mass fingerprint. The analytical method was applied to the analysis of gums from 12 other *Acacia* species and an attempt was made to find specific oligosaccharides that could be used to discriminate among them. Statistical analysis was performed to further explore the capability to differentiate these species. The implementation of a library of MALDI mass profiles of plant gums, with an initial focus on Acacia gums, represents the first MS-based attempt to facilitate reliable, species-level identification of these materials in unknown samples. The technique was successfully applied to the analysis of micro-samples from art objects of different types, with regard to geographical origin and date, including artefacts from ancient Egypt and a 20th century painting by Georges Braque, in the collections of The Metropolitan Museum of Art, New York, and the Art Institute of Chicago. Results demonstrated the possibility to detect Acacia gums from different species even in complex and aged micro-samples, providing important insights into the materials and condition of the objects. This research shows the potential to open new avenues of art historical and technical investigation into the specific plant sources, trade, and selection of materials by artists.

1. Introduction

Gum arabic, or Acacia gum, is the exudate generated onto the branches and trunk of *Acacia* trees as the result of a protection mechanism against insect, mechanical or microbial injury [1]. Among the more than one thousand *Acacia* species counted in the world, commercial gum arabic is obtained mainly from *A. senegal* (L.), which belongs to the *Vulgares* taxonomic series, and *A. seyal* (Del.) from the *Gummiferae* series [2]. *A. senegal* has been deeply studied since it comprises the majority of global trade [3], while *A. seyal* gained attention mainly in the last few decades following its acceptance as a food additive [4]. The major components of the two gums are hyperbranched polysaccharides that have a similar monosaccharide composition, characterized by the presence of D-Galactose (Gal), L-Arabinose (Ara), L-Rhamnose (Rha), D-Glucuronic acid and 4-*O*-methyl glucuronic acid; the gums also contain a minor protein fraction [5]. The two Acacia gums have a chain of 1,3 linked β-D-Galactopyranose (Gal*p*) units as core substituted by highly branched side chains in *A. senegal* and more linear, longer and less ramified branches in *A. seyal* [6,7] (Fig. 1). In terms of properties, *A. seyal* shows a greater average molecular weight than that of *A. senegal*, as well as lower intrinsic viscosity, less protein content, and lower surface activity [8–11].

Due to its high solubility and low viscosity, gum arabic has multiple applications mainly in the food industry as an emulsifier, stabilizer and thickener for confectionery, beverages, fruit-based foods and for flavour encapsulation [12]. It is also widely used for pharmaceutical [13], cosmetic, lithography, textile, printing and ceramics applications [14]. Authentication of gum arabic is a serious issue particularly in the food industry for quality control and trading [15] since gums obtained from *Acacia* species other than *A. senegal* and *A. seyal* are not commercially defined as Acacia gums [16]. Several methods can be used to identify gums from *A. senegal* and *A. seyal* and discriminate them from other

☆ Paper presented at TECHNART 2017 Conference, Bilbao (Spain), May 2–6, 2017.

* Corresponding author at: Natural History Museum of Denmark, University of Copenhagen, Øster Voldgade 5–7, 1350 København K, Denmark.
E-mail address: clara.granzotto@gmail.com (C. Granzotto).

https://doi.org/10.1016/j.microc.2018.08.058
Received 30 August 2017; Received in revised form 18 July 2018; Accepted 27 August 2018
Available online 30 August 2018
0026-265X/

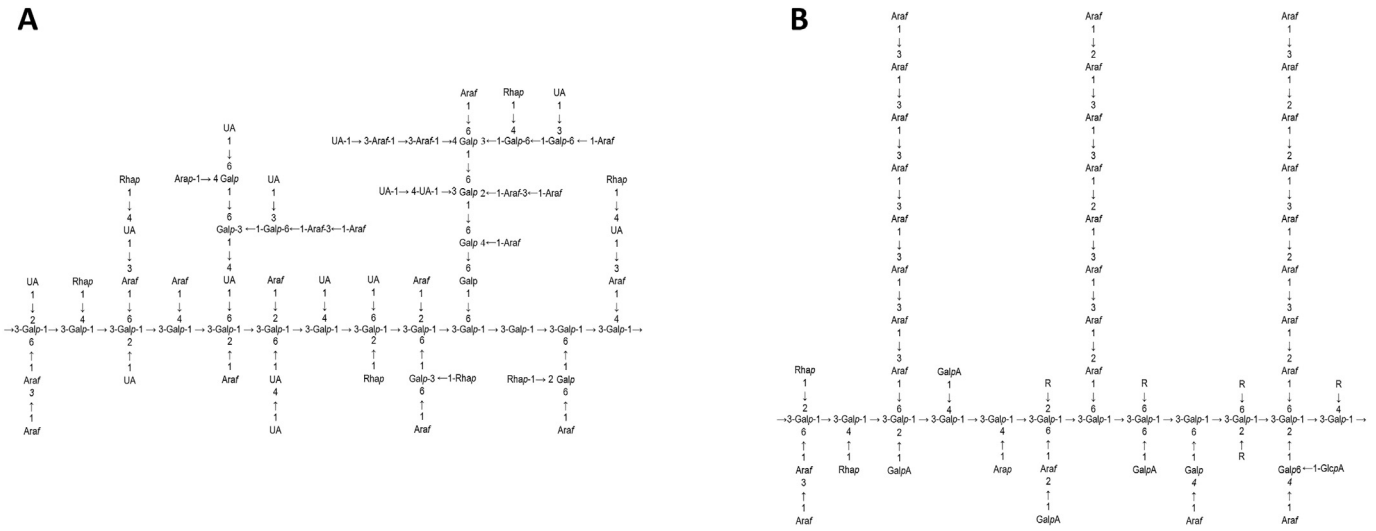

Fig. 1. Illustration of the suggested structures of the polysaccharide core of *A. senegal* (A) and *A. seyal* (B), (based on Nie et al. [6,7]).

Acacia gums used as food additives according to their physical/chemical properties: optical rotation, nitrogen content, ash content, moisture content, presence/absence of tannins, intrinsic viscosity, and sugar composition (determined by anion exchange chromatography) [17–19]. While these techniques are time-consuming and not highly sensitive, nuclear magnetic resonance (NMR) has been demonstrated as an effective technique in the discrimination of *A. senegal* and *A. seyal* [6,7] but it is rather inaccessible for industrial screening purposes. A rapid method based on near infrared (NIR) spectroscopy and chemometric analysis was recently developed for gum arabic authentication [20].

In the cultural heritage field the use of Acacia gums can be traced to as early as the 3rd millennium BCE in Ancient Egypt [21], and since the 18th century gum arabic has continued to be used as a medium for watercolor paints [22]. Analytical techniques such as gas chromatography/mass spectrometry (GC/MS) [23] and pyrolysis GC/MS (Py-GC/MS) [24] are the most widely used approaches to discriminate plant gum sources such as *Acacia* (gum arabic), *Astragalus* (tragacanth gum), *Sterculia urens* (karaya), *Anogeissus latifolia* (ghatti) and *Prunus* (cherry gum) based on their monosaccharide composition. In the literature the selective use of gums from different *Acacia* species in artists' materials is suggested [22,25] but to our knowledge it has never been analytically confirmed. In the analyses of a number of painted wooden objects and some stone objects from ancient Egypt in the Museum of Fine Arts, Boston, the use of gums from different *Acacia* species was suggested although it was not possible to discriminate between them using GC/MS [26]. The presence of gum from *A. nilotica* was suggested in samples from wall paintings from various sites in South India: analysis was performed by thin-layer chromatography and the exclusion of *A. senegal* or other *Acacia* species was based on the fact that *A. nilotica* is typical of the India region, not on differences in the analytical results from different Acacia gums [27]. In another study, the absence of rhamnose, as observed after GC/MS analysis of samples from paintings in the Tomb of Nefertari at Luxor, led to the conclusion that gum tragacanth was used [28]. However when gums from locally growing trees of the *Acacia* genus were analyzed, they too were found to be lacking in rhamnose, while the commercial gum arabic usually shows a rhamnose component. This indicated that the paint medium was likely gum arabic and not tragacanth, thus demonstrating the importance of characterizing gums from different species. A first systematic attempt to distinguish gums of different *Acacia* species was made by Lluveras et al. who performed analysis of *A. senegal*, *seyal*, *giraffe* and *karoo* [29]. The strategy, based on GC/MS analysis and a specific decisional scheme, allowed the differentiation of *A. senegal* from the other three species, but only when the nature of all of the other organic materials possibly present in the art samples is known (i.e. oils, resins, proteins). The presence of these other materials could hinder successful polysaccharide identification.

Matrix assisted laser desorption ionization-time-of-flight mass spectrometry (MALDI-TOF MS) has recently been shown to be a successful technique for the discrimination of the most common plant gums used in the cultural heritage field such as gum arabic (from *A. senegal*), cherry gum, locust bean gum and tragacanth gum [30]. The strategy involves partial enzymatic digestion of the polysaccharide, using specific glycoside hydrolases, followed by analysis of the released oligosaccharides by MALDI with tandem mass spectrometry (MALDI-TOF MS/MS). Due to significant differences in the polysaccharide structure, gums from different plant sources can be discriminated according to their unique saccharide mass fingerprint. The analytical strategy allows unambiguous identification of plant gums in aged microsamples, and has proved effective even in the presence of complex matrixes such as is typical for samples from works of art, due to the simultaneous presence of inorganic (e.g. pigment) and other organic components (e.g. resin, oil) [31,32].

In the present work, 47 samples of gum arabic from 14 different *Acacia* species, obtained from private, museum and botanical collections and commercial suppliers (see Table 1), were enzymatically digested and analyzed by MALDI-TOF MS following a previously developed protocol [30]. In particular, because of the commercial need to discriminate *A. senegal* from *A. seyal* and the other *Acacia* species, attention was focused on the detailed investigation of the MS profile of *A. seyal* by means of MALDI-TOF MS/MS experiments (the structure of gum from *A. senegal* has been addressed in detail in a previous publication [30]). Principal component analysis (PCA) and hierarchical clustering (HC) were performed: the application of statistical data analysis allowed for dimensional reduction and cluster assignment that helped to investigate the presence of patterns of ions associated with each *Acacia* species. In conjunction with analysis of the reference Acacia gums, the analytical strategy has been applied in the present work to elucidate the nature of organic materials in objects in the collections of The Metropolitan Museum of Art, New York (Met) and the Art Institute of Chicago (AIC), ranging from ancient Egyptian artefacts to 20th century paintings, and supplementing information gained by more established techniques such as Fourier transform infrared (FTIR) spectroscopy and Py-GC/MS. Due to uncertain provenance and sometimes limited numbers of available reference samples, some of the analytical findings reported must be considered tentative until a more comprehensive reference database is developed. Nonetheless, this work represents the first attempt using MALDI-TOF MS, and the first successful results demonstrating the qualitative discrimination of gums

from different *Acacia* species. This study confirms MALDI-TOF MS as a valuable analytical method to differentiate gums at the species level (*A. senegal* vs. *A. seyal*), as well as by genus (e.g. Acacia, Ceratonia) as reported in previous work [30].

2. Materials and methods

2.1. Chemicals and samples

Exo-β-1,3-galactanase (EC 3.2.1.145) and *endo*-β-1,4-mannanase (EC 3.2.1.78) were purchased from NZYtech. All other chemicals were purchased from Sigma-Aldrich. Full details of the reference Acacia gum samples analyzed in this study are provided in Table 1. Samples SEN_I, SEN_L, SEN_M, SEN_N, SEN_F, UNS_A, SEN_H, SEN_G, SEY_G, SEY_H, SEY_Q and SEY_I were obtained from the private collection of Prof. P. C. Ravines (details of individual suppliers are listed in the Table). Other samples were provided by Alland & Robert (Port-Mort, France), The Royal Botanic Gardens, Kew (London, UK) and The Field Museum of Natural History (Chicago, IL, USA). Objects from the Met's collection were analyzed: examples discussed in this paper are a coating on the *Kneeling statue of Amenemopetemhat*, Roman, Egyptian culture (664–610 BCE, No. 24.2.2), and *Figurines* (ca. 990–970 BCE, No. 25.3.155 a–d). From the AIC collections, samples of black and dark green paint from a late painting by Georges Braque, *Ajax* (1949/54, AIC No. 1997.447), and of red and yellow paints on a *Statue of Osiris* (Ptolemaic, 305–30 BCE, AIC No. 2002.542), are presented. The samples from works of art were not weighed but estimated to be less than few tens of micrograms.

Table 1
Details of the analyzed reference Acacia gum samples, family Leguminosae.

Sample	Species	Origin	Collection/supplier[1]
SEN_B	*A. senegal* (L.) Willd.	Asia, Pakistan, Balochistan	FM, acquired 1907
SEN_C	*A. senegal* (L.) Willd.	Africa, Sudan, Kordofan	FM, acquired 1907
SEN_D	*A. senegal* (L.) Willd.	Africa, Egypt	FM, acquired 1904
SEN_E	*A. senegal* (L.) Willd.	Asia, India	FM, acquired 1912
SEN_I[2]	*A. senegal* (L.) Willd.	Africa, Western Sudan	GA, collected 1994
SEN_L[2]	*A. senegal* (L.) Willd.	Africa, Southeast Sudan	GA, collected 1999
SEN_M[2]	*A. senegal* (L.) Willd.	Africa, Southeast Sudan	GA, collected 1994
SEN_N	*A. senegal* (L.) Willd.	Africa, Uganda	NRI
SEN_A	*A. senegal* (L.) Willd.	unknown	Zecchi
SEY_E	*A. seyal* Del.[3]	Africa, Niger	Kew, “tree no. 4”
SEY_C	*A. seyal* Del.	Africa, Niger	Kew, “tree no. 1”
SEY_B	*A. seyal* Del.	Africa, Niger	Kew, “tree no. 3”
SEY_D	*A. seyal* Del.	Africa, Niger	Kew, “tree no. 2”
SEY_N	*A. seyal* Del.	Africa, Tanzania	Kew, acquired 1904
SEY_F	*A. seyal* Del. var. seyal	Africa, Tanzania	Kew, acquired 1995
SEY_O	*A. seyal* Del.	Africa, Senegal	Kew, acquired 1995
SEY_P	*A. seyal* Del.	Africa, Sudan	Kew
SEY_G	*A. seyal* Del. var. fistula	Africa, Sudan, Khartoum	GA, collected 1999
SEY_H	*A. seyal* Del.var. seyal	Africa, Southeast Sudan	GA, collected 1997
SEY_A	*A. seyal* Del.	Unknown	FM, acquired 1995
SEY_Q	*A. seyal* Del.var. seyal	Unknown	CWSP
SEY_I	*A. seyal* Del.var. fistula	Unknown	CWSP
SEY_L	*A. seyal* Del.	Unknown	AR
STEN	*A. stenocarpa* Hochst. ex A. Rich.[4]	Africa, Egypt	FM
DEA_A	*A. dealbata* Link	Oceania, Australia, New South Wales	FM
DEA_B	*A. dealbata* Link	Unknown	Kew
DEC_A	*A. decurrens* Willd.	Oceania, Australia, New South Wales	FM, collected 1898
DEC_B	*A. decurrens* Willd. var. *mollis* Lindl.	Oceania, Australia, Tasmania	Kew
MEA	*A. mearnsii* De Wild.	Oceania, Australia, New South Wales	Kew
FER_A	*A. ferruginea* DC.	Asia, India	FM, acquired 1912
FER_B	*A. ferruginea* DC.	Asia, India, Madura	Kew
PEN_A	*A. penninervis* Sieber	Oceania, Australia, New South Wales	FM, collected 1898
PEN_B	*A. penninervis* Sieber	Oceania, Australia, New South Wales	Kew
FAR_A	*A. farnesiana* Willd.	Asia, India	FM, acquired 1912
FAR_B	*A. farnesiana* Willd.	Asia, India, Tamil Nadu	Kew
FAR_C	*A. farnesiana* Willd.	Asia, India, Tamil Nadu	Kew
NIL_A	*A. nilotica* (L.) Willd. ex Del.	Africa, South Africa, Natal	Kew
NIL_B	*A. nilotica* (L.) Willd. ex Del.	Africa, Egypt	Kew
POL	*A. polyacantha* Willd.	Africa, Nigeria	Kew
TOR	*A. tortilis* (Forssk.) Hayne	Unknown	Kew
ODO	*A. odoratissima* (L.f.) Willd.	Asia, India	FM, acquired 1912
VES	*A. vestita* Ker Gawl.	Oceania, Australia, New South Wales	FM, collected 1898
MIC	*A. microbotrya* Benth.	Oceania, Australia, New South Wales	FM, collected 1898
SEN_F	Gum arabic (unspecified)[5]	Africa, Sudan	JT
UNS_A	Gum arabic (unspecified)[6]	Asia, Israel, Jerusalem	JT
SEN_H	Gum arabic (unspecified)[5]	Africa, Kenya	Unknown supplier
SEN_G	Gum arabic (unspecified)[5]	Unknown	TNN, collected 1999

[1] Samples obtained from the following collections/suppliers: FM = The Field Museum, Chicago, IL, USA; GA = Gandil Agricultural Co. Ltd., Karthoum, Sudan (A. Karamallah); NRI = Natural Resources Institute, Chatham, UK (Sarah Taylor); Zecchi, Florence, Italy; Kew = Royal Botanic Gardens, Kew, UK; CWSP = Centre for Water Soluble Polymers, Wrexham, UK; AR = Alland & Robert, Port-Mort, France; JT = Jack Thompson, OR, USA; TNN = Tessa Neylan Nolan, Nakuru, Kenya.
[2] Analyzed in previous work [30].
[3] Currently described as *Vachellia seyal* (Delile) P.J.H.Hurter; applicable to all *A. seyal* Del. samples (see http://powo.science.kew.org).
[4] Synonymous with *A. seyal* Del.
[5] MALDI analysis indicates *A. senegal.*
[6] MALDI data could not be matched with any of the tested references.

2.2. Sample preparation and enzymatic digestion

Reference gum samples were solubilized in deionized water at a concentration of 1% w/v. An aliquot of each solution corresponding to around 1 mg of polysaccharide was collected, dried in a vacuum centrifuge at 30 °C (concentrator 5301, Eppendorf, Hamburg, Germany), and subjected to enzymatic digestion as described in a previous paper [30]. In summary, the dried polysaccharide sample was resolubilized in 100 μL of 50 mM phosphate buffer, pH 6, mixed vigorously and incubated with 100 mU of *exo*-β-1,3-galactanase for 5 h at 50 °C. If samples were not subjected immediately to digestion, they were dried and stored at −20 °C. All reference samples were run in triplicate. In the case of samples from museum objects, due to their limited amount (c. tens of μg) and complex composition, enzymatic digestion was performed directly on the samples without any previous extraction step. Due to the unknown nature of the polysaccharide material, samples were digested with a previously developed enzyme 'cocktail', a mixture of *exo*-β-1,3-galactanase and *endo*-β-1,4-mannanase [30]. The protocol has been optimized for low amounts of sample [32]. A volume of 50 μL of 50 mM phosphate buffer pH 7 was added to the sample together with 20 mU of each of the two enzymes, and digestion was carried out for 24 h at 45 °C. After centrifugation (13,400 rpm, 8 min) the supernatant was recovered, the enzymatic digestion quenched by heating at 100 °C for 15 min, and the solution dried in a vacuum centrifuge at 30 °C.

2.3. MALDI-TOF MS

The dried digested sample was resuspended in deionized water and several dilutions were prepared (c. 200–10 pmol). As the goal of this work was to provide a means for characterizing gums found in artworks with reference to a previously collected database, the matrix that provided the best ionization patterns, 3-aminoquinoline (3-AQ), was selected as described in previous work [30]. In summary, 0.5 μL of sample was mixed on the MALDI plate with 1 μL of 3-AQ, prepared 20 mg/mL in acetonitrile/water 1/2 (v/v), pH 5. Analyses were carried out at the Integrated Molecular Structure Education and Research Center (IMSERC), Northwestern University, IL, using a MALDI-TOF Autoflex III (Bruker) equipped with a tripled Nd:YAG laser, 355 nm wavelength, and at the Shared Instrumentation Facility 'SIF' at New York University, New York, NY, using a MALDI-TOF/TOF UltrafleXtreme (Bruker) equipped with a smartbeam™-II laser with 1000 Hz repetition rate. Spectra were obtained with a delayed extraction technology, in reflector positive mode with a grid voltage of 16 kV. A total of 3000 laser shots were accumulated for each spectrum. External calibration was performed using standard malto-oligosaccharides in the *m/z* range of 600–1300 Dalton (Da). MS/MS analyses were performed on a MALDI-TOF/TOF RapifleX (Bruker) at the Bruker Training Center in Billerica, Maine, in Collision-Induced Dissociation (CID) mode with argon. Data were analyzed using FlexAnalysis 3.0 software. Spectra were interpreted manually after baseline subtraction (TopHat algorithm, 10% minimal baseline width) and smoothing (Savitzky-Golay, 5 cycles).

2.4. FTIR

Analysis was performed with a Hyperion 2000 or 3000 FTIR microscope equipped with a mercury cadmium telluride (MCT) detector. A portion of each sample was crushed in a diamond anvil cell (Spectra Tech or Specac) and analyzed in transmission mode through the 15× objective. Acquisitions were performed in the range of 4000–600 or 4000–400 cm^{-1} at a resolution of 4 cm^{-1}. Each spectrum is the sum of multiple scans (128–256) according to the response of the different samples.

2.5. Py-GC/MS

Samples from works of art were placed in deactivated stainless steel pyrolysis cups (Eco-cup LF, Frontier lab). At the Met, analysis was performed with and without the addition to the sample of 3 μL of a 2.5% solution of tetramethylammonium hydroxide (TMAH) in methanol prior to insertion into a Frontier PY-2020iD vertical microfurnace pyrolyzer, with the furnace at 550 °C. The pyrolyzer is interfaced to the gas chromatograph (Agilent 6890) coupled with a single quadrupole mass spectrometer (Agilent 5973 Network Mass Selective Detector). The analysis was carried out in split mode 30:1 using a J&W DB-5MS or equivalent column (30 m × 0.25 mm × 0.25 μm). The inlet and MS transfer line were held at 320 °C. The carrier gas was helium, used at a constant flow of 1.5 mL/min. The GC oven temperature program was: 40 °C for 1 min, ramped to 320 at 10 °C /min, followed by 10 min isothermal period. Acquisition was performed in scan mode (*m/z* 40–600). Data analysis was performed on an Agilent MSD ChemStation D.02.00.275 and the NIST 2005 spectral libraries. A similar analytical protocol was used at AIC, but with the pyrolyzer interfaced to a Varian 3800 GC and Saturn 2200 ion trap MS. The GC split ratio was 10:1, column flow 1 mL/min, and MS transfer line 300 °C. The GC oven temperature program was: 40 °C for 2 min, ramped to 300 at 20 °C/min, followed by 10 min isothermal period. Data analysis was performed on the Varian MS Workstation.

2.6. Statistical analysis and machine learning

PCA was performed on the MALDI mass spectral data using the LAPACK implementation of the full singular value decomposition [33] and the scikit-learn Python package [34]. The mass spectral data were first transformed into a matrix with the columns representing *m/z* values, the rows representing all reference Acacia gum samples, and the entries representing the *s/n* for each ion. These values were scaled to a mean of zero and variance of 1 to avoid problems with differences in response between samples. There were a total of 250 ions present over the *m/z* range of 600–1300 Da in the mass spectra of all *Acacia* samples analyzed in this study, after filtering at a $s/n > 10$. Hierarchical clustering is a family of clustering algorithms that builds nested clusters by successive merging or splitting clusters; in this work the agglomerative clustering (AC) method, which builds clusters by merging, was employed [34]. For AC, low variance ions (those appearing in < 10% of samples) were excluded to reduce the dimensionality of the variables and improve clustering; this procedure removed 138 of 250 ions from the dataset. Several parameters control the fit in AC including the distance metric and the method for determining the distance between clusters called linkage. In addition to the number of clusters, the Hamming distance is used to determine the distance between values, and the average linkage is used to determine the distances between clusters. These parameters most closely preserved the pairwise distances in the original data as measured by the Cophenetic correlation coefficient (0.92). The goal of clustering is to find clusters present in the data without any other information. To improve the fit only the presence or absence of the ion was considered rather than the *m/z* values. To visualize the high-dimensional data, t-distributed stochastic neighbor embedding (t-SNE) was used. Without using this technique, a visualization of the 112 ions occurring in > 10% of the samples, each represented as a separate dimension, would not be possible. The t-SNE method represents the high-dimensional space of the 112 ions in two-dimensions using a

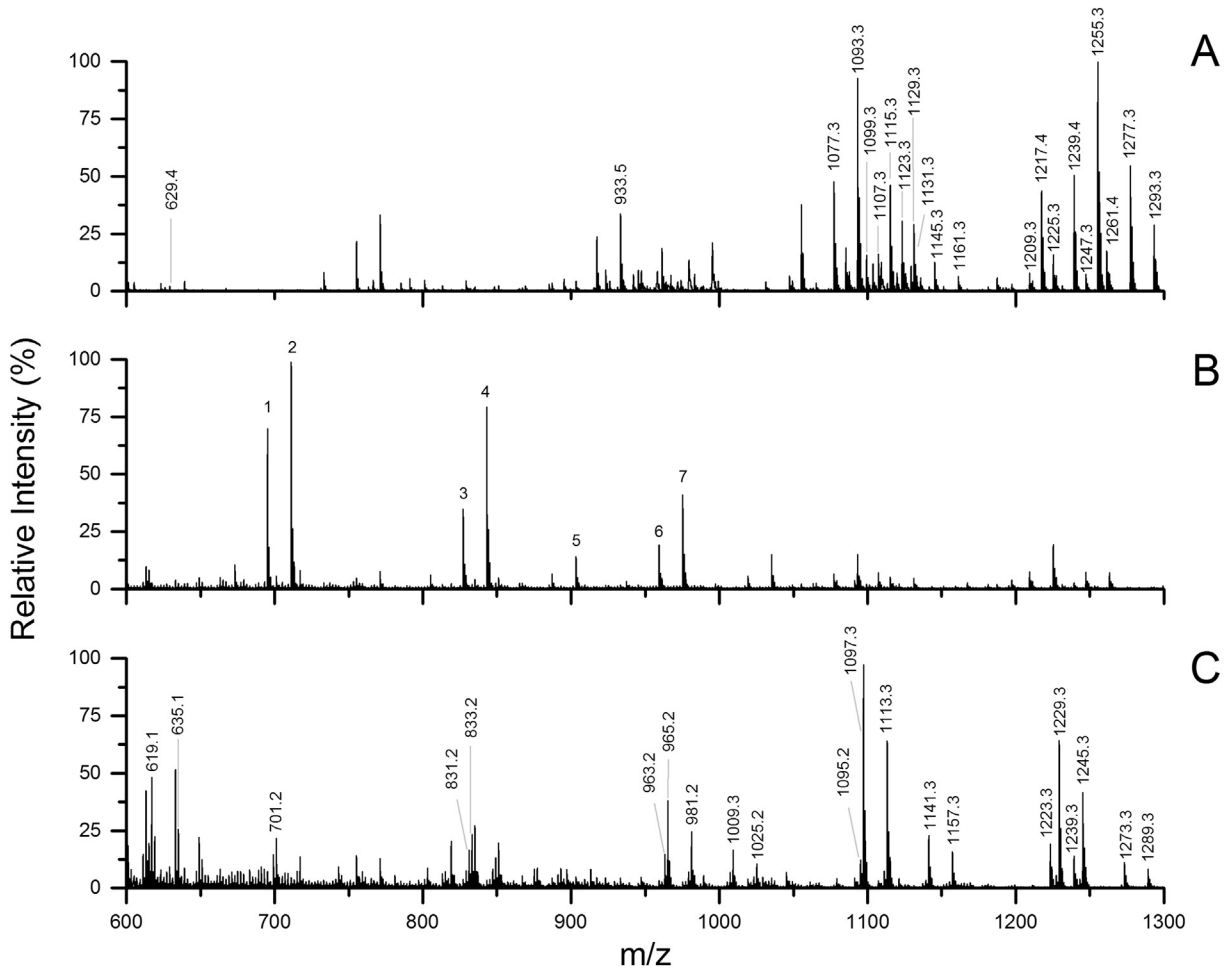

Fig. 2. Mass spectra from MALDI-TOF MS analysis of reference samples of (A) *A. senegal* (SEN_C); (B) *A. seyal* Del. (SEY_A) and (C) *A. tortilis* (TOR) enzymatically digested with *exo*-β-1,3-galactanase. Peak numbers for *A. seyal* refer to Table 2; *m/z* values for *A. senegal* and *A. tortilis* refer to Supplemental Table 1. Oligosaccharide attribution for *A. senegal* was detailed in previous work [30].

previously well described technique [35,36]. The most important parameter for t-SNE is perplexity, a measure of the balance between local and global structures in the data. The perplexity value used in this work is 5[1].

3. Results and discussion

3.1. Characterization of reference Acacia gums

3.1.1. MALDI-TOF MS and MS/MS analysis

Gums from 14 *Acacia* species (Table 1), including the most common *A. senegal* and *A. seyal*, were enzymatically digested and analyzed by MALDI-TOF MS as described in the Materials and Methods section. Representative mass fingerprints from examples of *A. senegal* (sample SEN_C), *A. seyal* Del. (sample SEY_A) and *A. tortilis* (sample TOR) covering the mass range of 600–1300 Da are shown in Fig. 2. The distinct differences in the mass profiles reflect the variation in the polysaccharide structure of the gums obtained from the different species. While these differences can be related to a known variance in the polysaccharide structure and composition when comparing *A. senegal* and *A. seyal*, as reported in Fig. 1, general hypotheses can be advanced for the other *Acacia* species. It is possible that the profiles are associated with differences in the monosaccharide composition [8], degree of branching, and/or length of side chains, resulting in characteristic oligosaccharides released during enzymatic digestion. Gum from *A. tortilis* for example, in contrast with *A. senegal* and *A. seyal*, contains a small amount of D-glucose and D-mannose [37]. Other examples are *A. nilotica* which has a higher number of arabinose units compared with galactose [38], while *A. mearnsii* has a lower uronic acid content compared to *A. senegal* as well as structural and molecular differences as suggested by tensiometry tests [39]. A table provided as supplemental material to this paper (Supplemental Table 1) lists characteristic ions with a *s/n* value above 10 that were consistently observed for the various *Acacia* species tested. Ions for A. *farnesiana* are not included in the table since consistent results were not generated from the references: the two samples FAR_B and FAR_C produced two different spectra, while no spectrum could be obtain for sample FAR_A. In this respect it should be stressed that the development of the sample database is work in progress. While the results for some species, such as *A. senegal* and *A. seyal*, can be interpreted with a degree of confidence since they are represented by a significant number of well-provenanced samples, others (such as *A. tortilis*) must be considered tentative at this stage since they are based on results from a few or just a single reference sample, and the reliability of the species attribution is sometimes uncertain, as discussed in more detail below.

Analysis of several gums from *A. senegal* confirmed its pattern, described in a previous publication [30], and allowed the successful

[1] The code used in this paper is available at: G. Ferguson, acacia gum maldi-tof, GitHub, 2018, https://github.com/gafergus/Art_Materials_Unsupervised_Machine_Learning.

categorization of ambiguous/unknown samples. As reported in Table 1, samples SEN_F, UNS_A, SEN_G and SEN_H were simply described as 'gum arabic', without any specification of the type of *Acacia*. Analysis of the samples confirmed three of the gums to be from the species *A. senegal*, whereas UNS_A could not be matched with any of the other gums tested. The latter sample, unusually for Acacia gums, was insoluble in water, an observation consistent with the MALDI data indicating a different type of gum. The MS profile of another sample described by the supplier as being from *A. senegal*, SEN_N, did not resemble the fingerprint for this species but instead showed similarities with results for *A. seyal*. Other problems with possible miscategorization of samples are discussed below in relation to the group of *A. seyal* samples studied. These results are an important demonstration that mistakes in the categorization or labelling of reference materials can occur and reinforces the critical need to develop a broad body of reference data.

Considering the data for *A. seyal* (Fig. 2B) in more detail, the oligosaccharidic fingerprint is dominated by ions with a mass difference of 132.4 Da, indicating the possible presence of side chains composed of pentosyl residues. Examination of the spectrum indicates that sodium and potassium adducts are present: for example the ion at *m/z* 673.2 (present at low intensity and not labeled in the figure) can be attributed to a protonated oligosaccharide $[M + H]^+$, followed by the corresponding sodium adduct $[M + Na]^+$, at *m/z* 695.2, and potassium adduct $[M + K]^+$, at *m/z* 711.2.

In order to confirm the composition of the oligosaccharides enzymatically released from *A. seyal* gum, CID-fragmentation experiments of the most intense and characteristic ions observed in the MS spectrum were performed. The mass spectra were dominated by a series of Y-ions due to the proton affinity of the quinoline matrix, which implies that the charge is retained by the fragments including the derivatized reducing end. Fragments were assigned using the Domon-Costello nomenclature [40]. The MS/MS spectrum of the ion at *m/z* 827.2, reported in Fig. 3, shows a series of Y-ions that allow attribution of the ion to the $Pent_5$ oligosaccharide (containing 5 pentose units). The fragment at *m/z* 299.0 indicates that the oligosaccharide is derivatized with 3-AQ and charged with Na^+. Based on the monosaccharides typically occurring in gums from *Acacia* species, the oligosaccharide may correspond to Ara_5 (5 arabinose units). MALDI-TOF MS/MS experiments allowed the composition of the most intense ions observed in the mass spectrum of *A. seyal* gum to be determined. Table 2 reports the identified characteristic ions, their mass and the assigned oligosaccharides.

Table 2
Experimental masses and assigned oligosaccharides for ions observed in MALDI-TOF MS analysis of gum from *A. seyal* (sample SEY_A); peak numbers refer to Fig. 2.

Peak no.	Experimental mass [Da]	Assignment
1	695.21	$Pent_4$ [3-AQ/M + Na]$^+$
2	711.18	$Pent_4$ [3-AQ/M + K]$^+$
3	827.24	$Pent_5$ [3-AQ/M + Na]$^+$
4	843.21	$Pent_5$ [3-AQ/M + K]$^+$
5	903.23	$Pent_3Hex_2$ [3-AQ/M + K]$^+$
6	959.27	$Pent_6$ [3-AQ/M + Na]$^+$
7	975.27	$Pent_6$ [3-AQ/M + K]$^+$

It is reported that plants of the same species grown in different locations produce gums that show different properties and chemical composition, which can be influenced also by factors such as the age of the tree and climatic conditions [41]. For this reason, to test the validity of the mass fingerprinting protocol for discriminating *A. seyal* gum from those of other *Acacia* species, various reference samples of *A. seyal* Del. were analyzed and their spectra compared to confirm the consistency of the MS profile. Nine samples out of the 14 listed in Table 1 produced the same MS profile as obtained for the sample SEY_A, thus supporting the validity of this profile as representative of *A. seyal*. One sample, SEY_L, has an MS profile that included all characteristic ions for *A. seyal*, but also a number of additional ions found in gum samples from

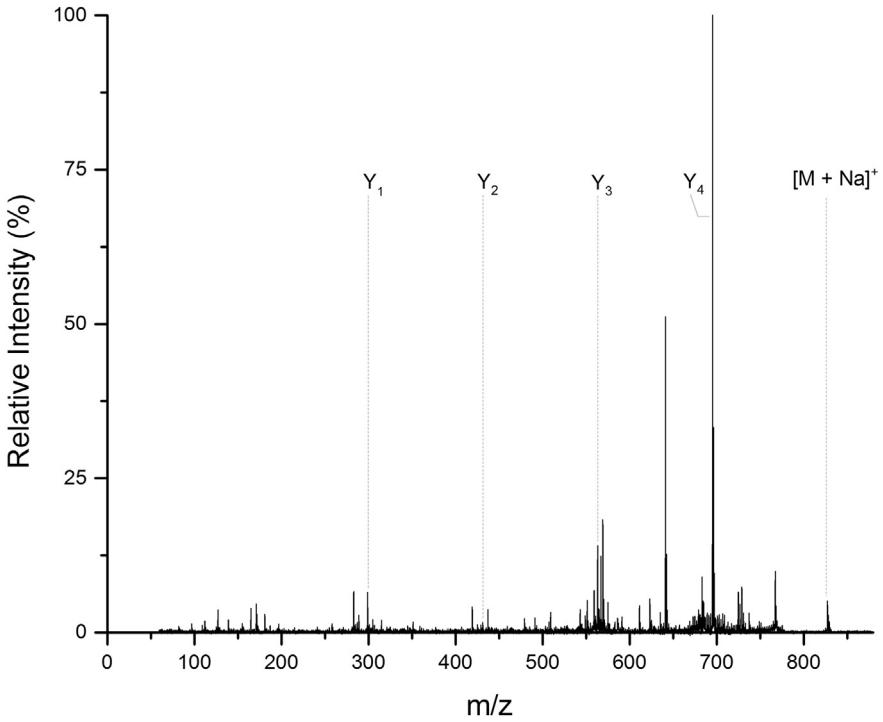

Fig. 3. MALDI-TOF MS2 spectrum of the ion $[3\text{-AQ/M} + Na]^+$ at *m/z* 827.2 from the digestion of gum from *A. seyal* with *exo*-β-1,3-galactanase. The fragmented Y-ions are observed.

other species: this result suggests that the sample may consist of a blend of gums from different sources, which is perhaps not surprising given that the material was obtained from a commercial supplier. In contrast, four samples, SEY_O, SEY_P, SEY_N and SEY_Q, show different profiles. More precisely, the mass spectra of SEY_N and SEY_Q resemble that obtained for a reference gum from *A. tortilis*, while spectra for SEY_O and SEY_P clearly resemble the saccharide fingerprint of *A. senegal*. It is possible that the reference samples were incorrectly attributed: sample SEY_Q, for example, is of unknown geographical origin; as opposed to samples from botanical collections it is more likely for samples used for industrial applications to lack a precise and recorded provenance.

Considering the samples that provided consistent results, distinct from the other species tested, attention was focused on the possible influence of location, tree and climatic conditions on the *A. seyal* MS profile. No differences were observed among samples SEY_E, SEY_C, SEY_B and SEY_D, which were all collected in Niger but from different trees. Furthermore, no significant differences due to the geographical area were observed in the MS profiles of the *A. seyal* samples. Regarding the different variants, samples SEY_G and SEY_I are described as gums from *A. seyal* Del. variant fistula while samples SEY_F and SEY_H are reported to come from the variant seyal. Beside the higher molecular weight of var. fistula, the two variants are characterized by a different monosaccharide composition [42,43]. This difference does not seem to affect the observed MS profile, however. The ions consistently observed in the majority of *A seyal* reference samples, and therefore used as characteristic marker ions for gums from this species, are listed in Table 2 and Supplemental Table 1. In summary, the results suggest that the *A. seyal* fingerprint does not vary significantly according to the area of collection or tree. However, the anomalies found in the set of 14 *A. seyal* samples once again stresses the necessity to be cautious in the interpretation of results, and especially with species for which a few or just a single reference sample is available.

3.1.2. Statistical analysis and machine learning

To understand the patterns of ions associated with each *Acacia* species in more detail, MALDI-TOF MS data for a subset of 34 of the reference samples were explored using PCA and HC (excluded from the analysis were samples that were inaccurately or ambiguously categorized, as discussed above, or that generated a poor signal). These statistical techniques allow for dimensional reduction in the case of PCA and cluster assignment in the case of HC. Using PCA, the mass spectral data were reduced to 20 principal components (PC) that explain 90% of the variance (see Section 2.6 for details of data treatment). All of the variance is explained at 27 PC (Supplemental Figs. 1 and 2). These large numbers make it difficult to determine the significance of the underlying data and so clustering was performed in addition to PCA; this is a method of unsupervised machine learning that finds patterns in data by grouping values with similar qualities. The final agglomerative clustering is shown in the dendrogram in Fig. 4A. The t-SNE method was used to visualize the high dimensional data in two-dimensional space, Fig. 4B. The t-SNE results show clustering of the samples similar to those obtained with AC though the techniques are unrelated.

The AC method allows the samples to be categorized as five clusters. These clusters can also be seen in the t-SNE. A first cluster includes *A. decurrens* (DEC_A), *A, odoratissima*, nine *A. seyal* samples, *A. stenocarpa*, *A. tortilis* and *A. vestita*. The grouping of *A. seyal* samples in the same cluster supports the idea that there are no major differences in their MS profiles related to factors such as the location of harvesting, consistent with the qualitative interpretations. The combination of *A. seyal* and *A. stenocarpa* in the same cluster is emblematic since, even if they were labeled with different names, *A. seyal* Del. and *A. stenocarpa* Hochst. ex A. Rich. are synonyms of the same species (see Table 1). One outlier from the *A. seyal* group is SEY_L, which is a cluster of its own (cluster 5). As discussed in Section 3.1.1, the MS data for this sample indicate that it may be a blend of gums from different *Acacia* species, which could account for its anomalous grouping: its positioning in the t-SNE plot, between clusters 1 and 3, tentatively suggests that it may include a gum from one of the *Acacia* species included in cluster 3 in addition to *A. seyal* gum (cluster 1). The AC method did not allow discrimination among the other *Acacia* species of the cluster, thus indicating that at this point in the research their profiles look similar and that analysis of more reference samples is necessary in order to identify possible characteristic ions.

Cluster 2 includes eight *A. senegal* samples, along with *A. nilotica* (NIL_B; the second sample of this species, NIL_A, was not included in the statistical analysis since the gum was only partially water-soluble and the obtained mass spectrum was unclear). Again, the occurrence of all *A. senegal* samples in a single group supports the visual assessment of similarity in the MS data, and indicates that they are distinct from many of the other species. Cluster 3 comprises *A. dealbata*, *A. decurrens* (DEC_B), *A mearnsii*, *A. microbotrya* and *A. penninervis*. These species cannot be further discriminated at this stage of the research. It should be noted that the two samples of gum from *A. decurrens*, DEC_A and DEC_B, occur in two different clusters, 1 and 3. Considering the botanical information available for the samples (Table 1), it is possible to suppose that their profiles show differences due to the fact that DEC_B is from a specific variant of *A. decurrens*. However, a greater number of samples from A. *decurrens* would be necessary to drive any firm conclusion. Finally, cluster 4 includes samples from *A. ferruginea* and *A. polyacantha*.

In conclusion, while AC and t-SNE are independent methods, they show similar groupings in the data. The correspondence of these methods indicates a persistence of the groupings, strengthening their validity. Statistical analysis thus proved to be a useful tool to simplify the mass spectrometric data set and clarify differences/similarities among the *Acacia* species profiles. This strategy was subsequently applied to samples from works of art to aid in the interpretation of the MALDI data.

3.2. Applications to samples from works of art

The ability to discriminate gums from different *Acacia* species, as demonstrated by the analyses of references, is potentially valuable to address questions relating to artists' preferences in the use of materials, their availability, the existence of trade relationships, and the provenance in the use of gums in ancient and modern artefacts. As previously pointed out, for example, making assumptions about a gum's source based on locally available *Acacia* species can be misleading. The MS profiles generated from reference sample data and the clustering strategy outlined above were applied to characterize Acacia gums in samples from works of art dating from the first century BCE to the 1950s. Results for museum objects analyzed to date are summarized in Table 3, and selected examples are described below to highlight unexpected findings as well as challenges in the interpretation of data.

3.2.1. Artefacts from ancient Egypt

A sample from an Egyptian *Figurine* in the collection of the Met (No. 25.3.155 c) was first investigated by FTIR. The figurine is one of a group found inside the mummy of a wealthy woman and they represent the Four Sons of Horus, who protected the four internal organs that were removed during mummification [44]. FTIR results indicated the presence of a polysaccharide material (Supplemental Fig. 3) that was also confirmed by Py-GC/MS with and without sample derivatization by TMAH. Evidence for a plant gum was based on the detection of compounds such as 2-furancarboxaldehyde in the non-derivatized sample [45] along with 1,2,4-trimethoxybenzene and methylated monosaccharide derivatives in the sample treated with TMAH [46]. Py-GC/MS of the derivatized sample also revealed the presence of a drying oil, as indicated by the presence of methylated derivatives of fatty acids such as palmitic, stearic, azelaic, and suberic (Supplemental Fig. 4). However, since Py-GC/MS does not allow unambiguous discrimination of different carbohydrates, the optimized MALDI mass fingerprinting

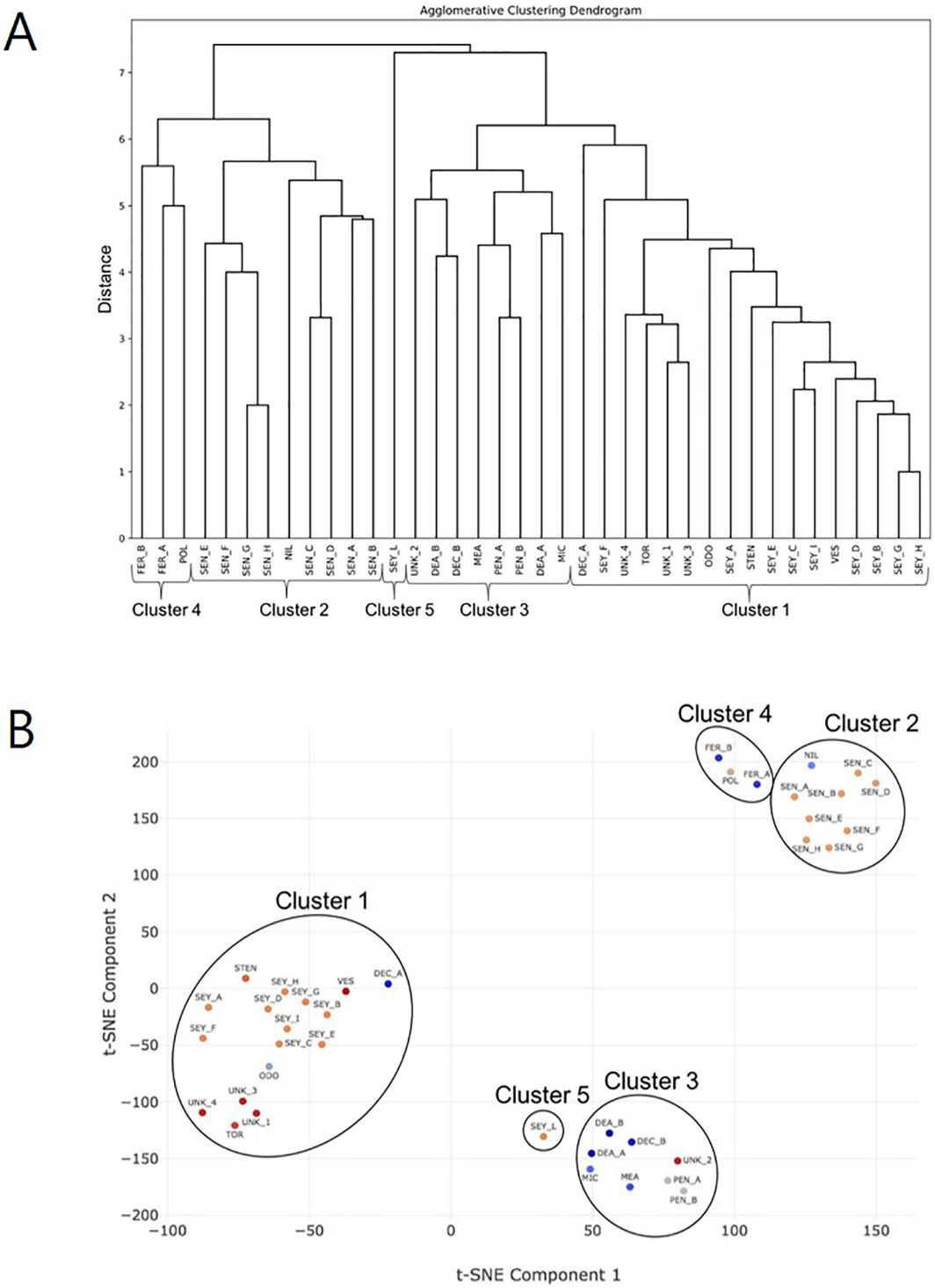

Fig. 4. (A) Agglomerative clustering dendrogram; parameters chosen were Hamming distances with average linkage. (B) Manifold learning using the t-distributed stochastic neighbor embedding (t-SNE) with a perplexity of 5 to visualize the sample distribution in two-dimensional space. The circles represent the AC clusters. Samples UNK_1-4 refer to analyses of works of art discussed in Section 3.2.

strategy was used to further investigate the saccharide component. The sample was digested with the enzyme 'cocktail' without any previous extraction, as described in Section 2.2. The mass spectrum of the sample from the Egyptian figurine is shown in Fig. 5A.

MALDI-TOF MS analysis allowed the detection of characteristic oligosaccharide ions, despite the presence in the sample of drying oil, highlighting the effectiveness of the procedure in the presence of additional organic materials and without a clean-up step [32]. Examination of the spectrum indicated that the most intense ions are K cation adducts that follow the less intense Na cation adducts. Mass intervals of 132 Da between the ion series correspond to pentoses, thus aiding the attribution of the unknown organic material to an Acacia gum, although different from *A. senegal*. According to AC results, the figurine sample (UNK_3) was included in cluster 1 (see Fig. 4). In comparison with the reference samples analyzed to date, the MS spectrum shows two prominent ions, *m/z* 1113.3 and 981.2 that are in

Table 3
Summary of works of art from the Met and AIC's collections analyzed by MALDI-TOF MS, and *Acacia* species attribution based on closest matches with the current database.

Object	Date	Sample	Interpretation
Figurines (Met No. 25.3.155 c)	ca. 990–970 BCE	Bulk material	*A. tortilis*
Kneeling statue of Amenemopetemhat (Met No. 24.2.2)	664–610 BCE	Coating	*A. dealbata, A. decurrens, A. mearnsii, A. microbotrya,* or *A. penninervis*
Statue of Osiris (AIC No. 2002.542)	305–30 BCE	Red and yellow paint	*A. tortilis*
J. S. Sargent, *Olive Trees, Corfu* (AIC No. 1933.505)	1909	Matte watercolor medium	*A. senegal*
J. S. Sargent, *The Basin, Vizcaya* (AIC No. 309.1996)	1917	Glossy watercolor medium	*A. senegal*
J. S. Sargent, *The Terrace, Vizcaya* (AIC No. 311.1996)	1917	Matte watercolor medium	*A. senegal*
Georges Braque, *Ajax* (AIC No. 1997.447)	1949/54	Matte black paint	*A. senegal*
		Dark green paint	*A. tortilis*, *A. penninervis*, *A. mearnsii*, or *A. polyacantha*
Walker Evans, *Anna Maria, Florida* (Met No. 1994.261.178)	1958	Green paint	*A. senegal*

common with the reference *A. tortilis*, and only one, *m/z* 717.2, with *A. Stenocarpa* or *A. polyacantha* (Supplemental Table 1). The AC results suggest closer similarity with *A. tortilis* (also in cluster 1), but since this conclusion is based on comparison with only one *A. tortilis* reference spectrum, and only 2 ions are shared, the attribution to this species is tentative. *A. tortilis* has been reported to be among species that commonly occurred in ancient Egypt [25], as well as today. Since there are more than one hundred *Acacia* species among the African flora [47], and not all of them have yet been analyzed, confirmation of this interpretation will rely on expansion and validation of the reference database. However, this result is an important indication that species different from the most widespread *A. senegal* and *seyal* might have been used by artists at that time.

The same analytical strategy was applied to study the painting materials of a wooden statue of the Egyptian god Osiris of the Late Ptolemaic period in the collection of the AIC (No. 2002.542) (Fig. 6), an object that was previously analyzed non-invasively using X-ray fluorescence (XRF), FTIR and Raman spectroscopy, to better understand the painting technique and to obtain information about the pigments and binding medium [48]. FTIR analysis indicated the use of a polysaccharide (plant gum) as the binder for red and yellow paints made, respectively, with cinnabar (mercuric sulfide) and pararealgar (arsenic sulfide) pigments; these areas of paint were curiously cracked and flaking away from the surface, showing the white ground layer underneath, and so a detailed characterization of the binding medium was of interest. Samples of red and yellow paint were digested without any previous extraction of the polysaccharide binder in water, due to the extremely limited amount (a few tens of micrograms at most). The mass spectrum obtained for the red sample is shown in Fig. 5B. As in the sample from the figurine, the mass difference of 132 Da between the most intense series of ions is indicative of a gum from *Acacia* trees. Application of AC again resulted in the inclusion of the sample (UNK_1) in cluster 1, and the paired Na and K adduct cations with, respectively, *m/z* 965.1 and 981.2, 1097.1 and 1113.3, 1239.1 and 1245.1, show close resemblance to the reference spectrum for *A. tortilis*. Comparison of the mass spectra of the figurine (Fig. 5A) and the red sample from Osiris statue (Fig. 5B) indicate that, as noted above, differences in the relative ion abundances can occur, and this may be the reason for the apparently poor correspondence between data for the figurine sample with reference spectra. While the relative ion abundance obtained with MALDI-TOF MS is not highly reproducible, however, the final interpretation is the same. A similar profile, although with lower intensity ions, was also observed for the yellow sample from the Osiris statue, supporting the possible plant gum attribution. While caution must again be stressed in this interpretation since it is based on comparison with just one reference sample, the use of an unusual medium such as *A. tortilis*, which contains just a 4% water insoluble fraction [37], instead of the completely water soluble *A. senegal,* might have some connection with the brittleness and flaking observed in the paint layers.

Regarding another object in the collection of the Met, the *Kneeling statue of Amenemopetemhat* (No. 24.2.2) (Fig. 7, left) [49], analyses were performed on a thin, water-soluble coating layer that was observed during a conservation treatment. The coating was present on the polished surface as well as in areas with losses (e.g. the neck and right hand). Analysis by FTIR of a water-extracted sample showed the coating to be a polysaccharide gum-based material (Supplemental Fig. 5). Due to the limited thickness of the coating layer, no samples could be taken from the statue surface and only the cotton swabs used during conservation testing for coating removal were available for analysis. For this reason a modified sample preparation strategy for MALDI-TOF MS analysis was developed: the cotton swabs were inserted in a 600 μL Eppendorf tube, 100 μL of 50 mM phosphate buffer pH 7 were added, and digestion performed as described previously. In order to rule out the possible influence of contamination, a clean cotton swab was also analyzed as a blank control and its mass spectrum compared with the spectrum of the coating sample. Results showed that the cellulose-based cotton did not interfere with the enzymatic digestion of the coating sample, thus further demonstrating how the analytical strategy is gum-specific and, in contrast with the more widely used GC/MS strategy [23], does not appear to be affected by the presence of other organic components. The mass spectrum of the coating sample (Fig. 7, right) was characterized by the presence of both Na and K adduct cations. The coating sample (UNK_2) was included in cluster 3 by AC and t-SNE; this group includes *A. dealbata*, *A. decurrens*, *A. mearnsii*, *A. microbotrya* and *A. penninervis*. Comparison of the MS fingerprint and the most intense ions of the sample spectrum with the reference gum profiles analyzed to date supported the AC result. Since for all the gums in this group only one or two references of the species have been analyzed, interpretation of the coating sample is limited to the general group of Acacia gums included in the cluster. The same result was obtained for samples both from the polished surfaces and from areas with losses, supporting the conclusion that the coating was not original but had likely been added during a previous conservation treatment for esthetic reasons. However, in a typical treatment the presence of *A. senegal* would be expected since this is the most commonly used gum in conservation laboratories. While the interpretation of the use of a gum from one of these species must again be made with caution, because of the limited number of references available, the significance of the use of Acacia gum from a different, less widespread species is still unclear.

3.2.2. A painting by Georges Braque

In another case study, this time from the 20th century, the MALDI-TOF MS strategy was applied to investigate paint media used by Georges Braque (1882–1963) in his late painting *Ajax* (1949/54, AIC No. 1997.447) (Fig. 8, left). Analysis of paint samples by FTIR and Py-GC/MS with TMAH had indicated the use of drying oil with Pinaceae resin, in some areas combined with a plant gum [50]. As described in Section 3.2.1 above, however, these techniques do not allow the precise discrimination of polysaccharide materials. Previously reported analysis by MALDI-TOF MS of a matte black paint, containing predominantly carbon black pigment, showed the presence of a gum from *A. senegal* thus confirming that the artist combined oil-based and water-based media in this painting [32]. For a dark green paint sample, containing Prussian blue and yellow ochre pigments, a different gum pattern was obtained after enzymatic digestion: the mass spectrum, shown in Fig. 8, exhibited several ions in common with those found for reference samples of *A. tortilis*, *A. penninervis, A. mearnsii* and *A. polyacantha*. AC classified the sample (UNK_4) in cluster 1, along with *A. tortilis*. A preliminary report of this analysis suggested that the sample may contain gum from *A. seyal* [32], also grouped in cluster 1, but this interpretation has been revised following analysis of a larger number of gums from *A. seyal* and other *Acacia* species (see discussion in Section 3.1 above), and once again stresses the need for a broad reference database in order to draw reliable conclusions regarding plant sources.

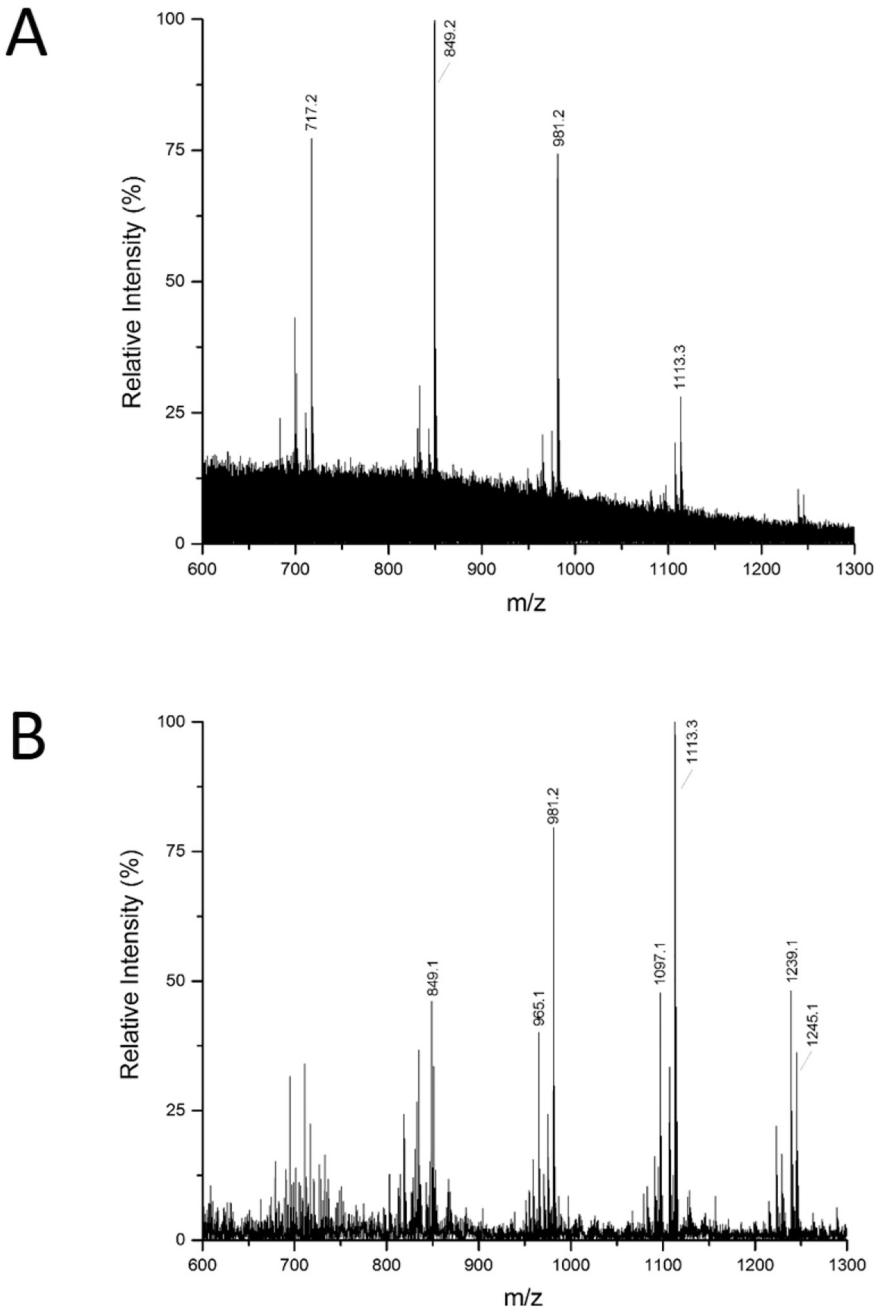

Fig. 5. Mass spectra from MALDI-TOF MS analysis of (A) sample from Egyptian figurine (Met) and (B) red paint sample from the *Statue of Osiris* (AIC), both enzymatically digested with *exo*-β-1,3-galactanase and *endo*-β-1,4-mannanase. Only the *m/z* values of the diagnostic ions with a *s/n* value greater that 10 are indicated in the spectra.

Fig. 6. *Statue of Osiris*. Egyptian, Ptolemaic Period (4th–1st century BCE). Wood with ground layer, pigment, gilding, and textile; h. 62.9 cm (24 1/4 in.). Gift of Phoenix Ancient Art, S.A., 2002.542.

The low *s/n* obtained in this case did not allow for a confident discrimination among the assignations but the result nonetheless provides evidence for the presence of gum from a second *Acacia* species in addition to *A. senegal*, or possibly a mixture of gums. Further study of examples of modern paint materials will also be valuable to extend our body of comparative data and to determine the variety of gums used to formulate water-based paint media, which may in turn relate to factors such as cost, variable supply, or adulteration of materials.

4. Conclusion

The results of this study indicate that gums from *A. senegal* and *A. seyal* can be distinguished from their mass fingerprints, representing patterns of specific oligosaccharides produced by enzymatic digestion and subsequent MALDI-TOF MS analysis. In the case of gum from *A. seyal*, further analysis by MALDI-TOF MS/MS analysis allowed determination of the composition of the most intense ions observed in the mass spectrum, resulting in more detailed knowledge of the gum's chemical structure. In addition, gums analyzed from 12 other *Acacia* species showed distinctive and characteristic MS fingerprints, thus further demonstrating the potential of MALDI-TOF MS to provide species-specific information. The analytical approach was successfully applied to the analysis of complex micro-samples from works of art, including artefacts from ancient Egypt as well as examples from the twentieth century, and provided direct analytical evidence for the first time of gums from different *Acacia* species in museum objects, including the most widely encountered *A. senegal*, but also other less common examples. Due to the limited number of reference plant gums analyzed so far, and considering the diverse range of species of *Acacia* and other plants that are known to produce polysaccharide gums, the results presented from case studies must be considered tentative, and firm conclusions about the plant species will require further expansion of the comparative database. Continuing research to extend the mass profile database and investigate the underlying structural differences will lead to a library of MALDI mass fingerprints that will facilitate reliable identification and differentiation of plant gums. Nevertheless, this research represents the first attempt to distinguish gums from different *Acacia* species by MALDI-TOF MS, and has proven successful even for aged material in the presence of other organic or inorganic material. Ultimately, this robust analytical approach should be of great benefit for the analysis of plant gums, both in cultural heritage and in other areas of polysaccharide research.

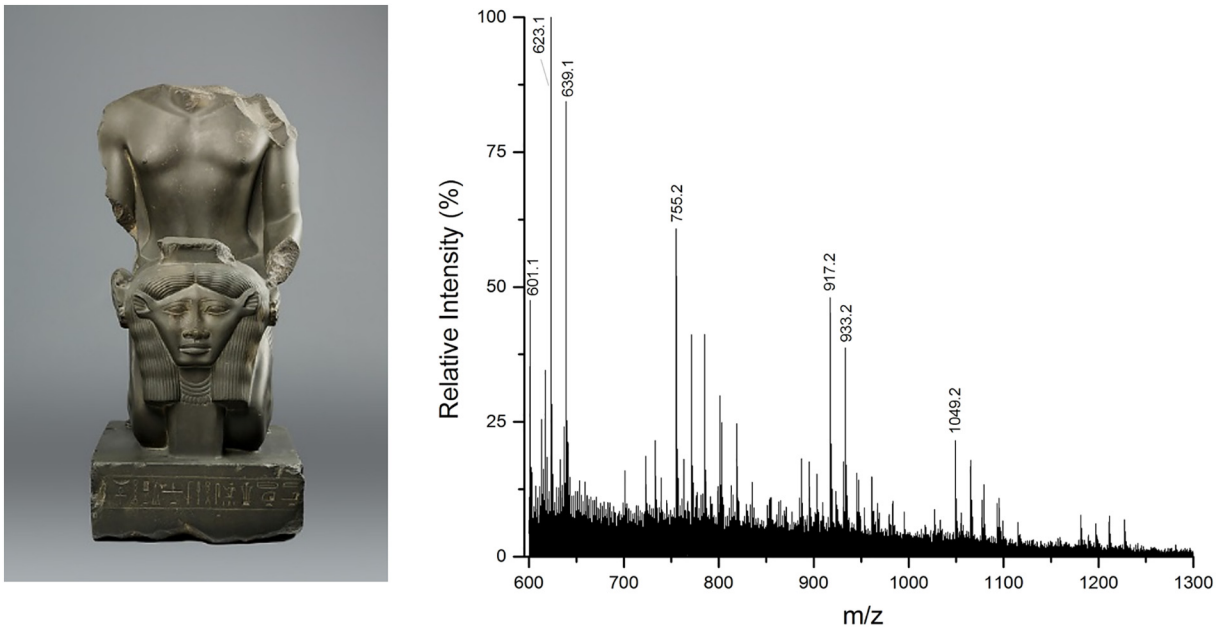

Fig. 7. Left: *Kneeling statue of Amenemopetemhat.* Egyptian, Late Period, Saite (664–610 BCE). Meta-Greywacke; h. 64.5 cm (25 3/8 in.). Rogers Fund, 1924, 24.2.2. Right: mass spectrum of the coating layer. Sample was enzymatically digested with *exo*-β-1,3-galactanase and *endo*-β-1,4-mannanase. Only the *m/z* values of the diagnostic ions with a *s/n* value > 10 are indicated in the spectrum.

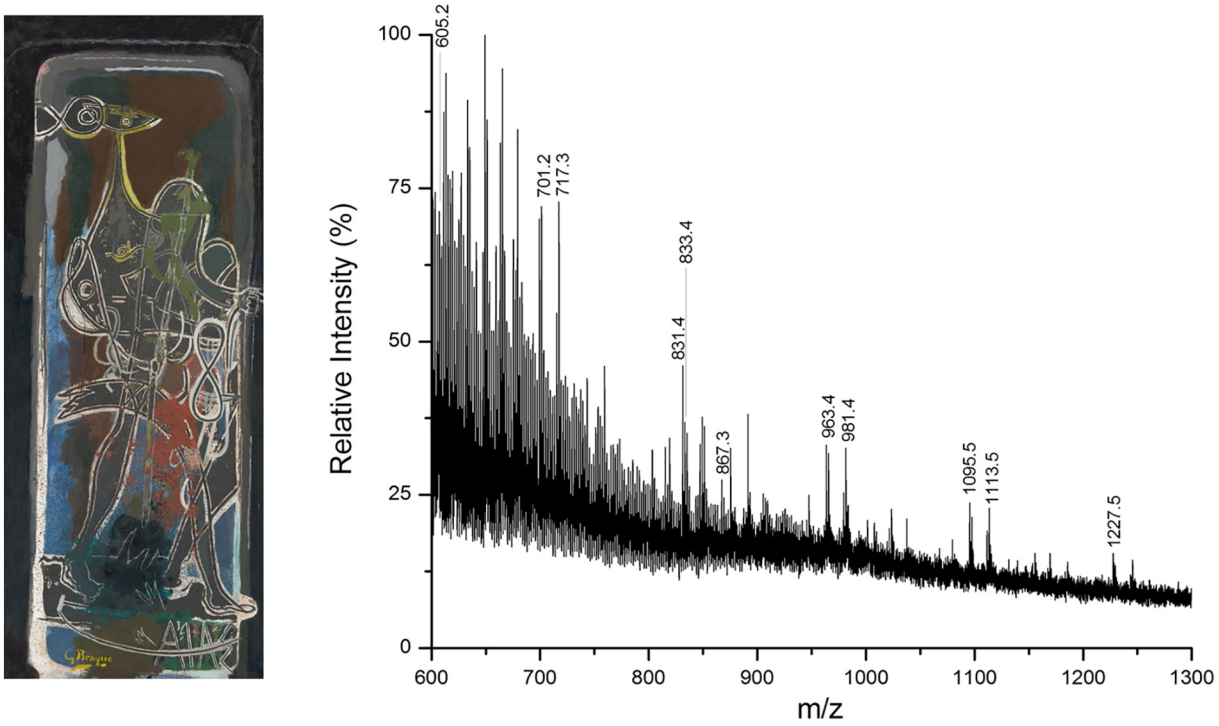

Fig. 8. Left: Georges Braque, *Ajax*, 1949/54, oil and mixed media on paper mounted on canvas, 179 cm × 71 cm, Bequest of Florene May Schoenborn, Art Institute of Chicago no. 1997.447, Copyright 2016 Artists Rights Society (ARS), New York/ADAGP, Paris. Right: mass spectrum of the dark green paint. Sample was enzymatically digested with *exo*-β-1,3-galactanase and *endo*-β-1,4-mannanase. The *m/z* values of diagnostic ions are indicated in the spectrum.

Acknowledgements

The research was made possible thanks to a visiting research scholarship at the Northwestern University/Art Institute of Chicago Center for Scientific Studies in the Arts (NU-ACCESS), funded through a grant from the Andrew W. Mellon Foundation; and to a postdoctoral fellowship at The Metropolitan Museum of Art, New York, also funded by the Andrew W. Mellon Foundation. The Bruker MALDI-TOF TOF UltrafleXtreme MS Spectrometer at the SIF facility at NYU was acquired through the support of the National Science Foundation under Award Number CHE-0958457. Francesca Casadio and Allison Langley at the Art Institute of Chicago, and Marc Walton, S. Habibi Goudarzi, Saman Shafaie, and Paul Thomas at Northwestern University are thanked for their support and contributions. Paul Kowalski and Ju Yue at the Bruker training center in Billerica (MA) are thanked for the MS/MS analyses. Frances Cook at The Royal Botanic Gardens, Kew; Christine Niezgoda at The Field Museum of Natural History, Chicago; and Prof. P. C. Ravines, Director and Associate Professor of the Art Conservation Department of The State University of New York, Buffalo State; are thanked for providing reference Acacia gums. The authors also gratefully acknowledge Anna Serotta (Department of Object Conservation, The Metropolitan Museum of Art) and Diana Craig Patch (Department of Egyptian Art, The Metropolitan Museum of Art) for providing samples from works of art.

This research did not receive any specific grant from funding agencies in the public, commercial, or not-for-profit sectors.

Appendix A. Supplementary data

Supplementary data to this article can be found online at https://doi.org/10.1016/j.microc.2018.08.058.

References

[1] P.A. Williams, G.O. Phillips, Gum Arabic, Handbook of Hydrocolloids, CRC Press, New York, NY, 2000, pp. 252–273.
[2] FAO, Gum Arabic, Rome, (1999).
[3] C. Sanchez, M. Nigen, V. Mejia Tamayo, T. Doco, P. Williams, C. Amine, D. Renard, Acacia Gum: History of the Future, Food Hydrocolloids, (2017), https://doi.org/10.1016/j.foodhyd.2017.04.008.
[4] FAO/WHO, Combined Compendium of Food Additive Specifications, Rome, (2006), p. 296.
[5] L. Lopez-Torrez, M. Nigen, P. Williams, T. Doco, C. Sanchez, Acacia senegal vs. Acacia seyal gums – part 1: composition and structure of hyperbranched plant exudates, Food Hydrocoll. 51 (2015) 41–53.
[6] S.-P. Nie, C. Wang, S.W. Cui, Q. Wang, M.-Y. Xie, G.O. Phillips, The core carbohydrate structure of *Acacia seyal* var. seyal (Gum arabic), Food Hydrocoll. 32 (2013) 221–227.
[7] S.-P. Nie, C. Wang, S.W. Cui, Q. Wang, M.-Y. Xie, G.O. Phillips, A further amendment to the classical core structure of gum arabic (Acacia Senegal), Food Hydrocoll. 31 (2013) 42–48.
[8] S. Al-Assaf, G.O. Phillips, P.A. Williams, Studies on Acacia exudate gums: part II. Molecular weight comparison of the Vulgares and Gummiferae series of Acacia gums, Food Hydrocoll. 19 (2005) 661–667.
[9] M. Elmanan, S. Al-Assaf, G.O. Phillips, P.A. Williams, Studies on *Acacia* exudate gums: part VI. Interfacial rheology of *Acacia senegal* and *Acacia seyal*, Food Hydrocoll. 22 (2008) 682–689.
[10] C. Flindt, S. Al-Assaf, G.O. Phillips, P.A. Williams, Studies on acacia exudate gums. Part V. Structural features of *Acacia seyal*, Food Hydrocoll. 19 (2005) 687–701.
[11] N.E. Siddig, M.E. Osman, S. Al-Assaf, G.O. Phillips, P.A. Williams, Studies on acacia exudate gums, part IV. Distribution of molecular components in *Acacia seyal* in relation to *Acacia senegal*, Food Hydrocoll. 19 (2005) 679–686.
[12] F. Thevenet, Acacia Gum (Gum Arabic), Food Stabilisers, Thickeners and Gelling Agents, Wiley-Blackwell, 2009, pp. 11–30.
[13] S. Patel, A. Goyal, Applications of natural polymer gum Arabic: a review, Int. J. Food Prop. 18 (2015) 986–998.
[14] D. Verbeken, S. Dierckx, K. Dewettinck, Exudate gums: occurrence, production, and applications, Appl. Microbiol. Biotechnol. 63 (2003) 10–21.
[15] K.M. Sørensen, B. Khakimov, S.B. Engelsen, The use of rapid spectroscopic screening methods to detect adulteration of food raw materials and ingredients, Curr. Opin. Food Sci. 10 (2016) 45–51.
[16] G.O. Phillips, P.A. Williams, G.O. Phillips, P.A. Williams (Eds.), Handbook of Hydrocolloids, CRC Press, New York, NY, 2009.
[17] I.B. Gashua, P.A. Williams, M.P. Yadav, T.C. Baldwin, Characterisation and molecular association of Nigerian and Sudanese Acacia gum exudates, Food Hydrocoll. 51 (2015) 405–413.
[18] I.B. Gashua, P.A. Williams, T.C. Baldwin, Molecular characteristics, association and interfacial properties of gum Arabic harvested from both *Acacia senegal* and *Acacia seyal*, Food Hydrocoll. 61 (2016) 514–522.
[19] P. Jurasek, S. Varga, G.O. Phillips, Classification of natural gums. VII. Relationships between the series Vulgares (*Acacia senegal*) and Gummiferae (*Acacia seyal*), Food

Hydrocoll. 9 (1995) 17–34.
[20] Y. Dong, K.M. Sørensen, S. He, S.B. Engelsen, Gum Arabic authentication and mixture quantification by near infrared spectroscopy, Food Control 78 (2017) 144–149.
[21] A. Lucas, Ancient Egyptian Materials and Industries, London, (2003).
[22] B.A. Ormsby, J.H. Townsend, B.W. Singer, J.R. Dean, British watercolour cakes from the eighteenth to the early twentieth century, Stud. Conserv. 50 (2005) 45–66.
[23] A. Lluveras-Tenorio, J. Mazurek, A. Restivo, M.P. Colombini, I. Bonaduce, The development of a new analytical model for the identification of saccharide binders in paint samples, PLoS One 7 (2012) E49383.
[24] C. Riedo, D. Scalarone, O. Chiantore, Multivariate analysis of pyrolysis-GC/MS data for identification of polysaccharide binding media, Anal. Methods 5 (2013) 4060–4067.
[25] R. Newman, M. Serpico, Adhesives and Binders, Ancient Egyptian Materials and Technology, University Press, Cambridge, Cambridge, 2000.
[26] R. Newman, S.M. Halpine, The binding media of ancient Egyptian painting, in: W.V. Davie (Ed.), Colour and Painting in Ancient Egypt, British Museum Press, London, 2001.
[27] B.V. Kharbade, G.P. Joshi, Thin-layer chromatographic and hydrolysis methods for the identification of plant gums in art objects, Stud. Conserv. 40 (1995) 93–102.
[28] P. Mora, L. Mora, E. Porta, K. Grimstad (Ed.), ICOM Committee for Conservation, Dresden, 1990, p. 518.
[29] A. Lluveras-Tenorio, J. Mazurek, A. Restivo, M.P. Colombini, I. Bonaduce, Analysis of plant gums and saccharide materials in paint samples: comparison of GC-MS analytical procedures and databases, Chem. Central J. 6 (2012) 115.
[30] C. Granzotto, J. Arslanoglu, C. Rolando, C. Tokarski, Plant gum identification in historic artworks, Sci. Rep. 7 (2017) 44538.
[31] C. Granzotto, J. Arslanoglu, Revealing the binding medium of a Roman Egyptian painted mummy shroud, J. Cult. Herit. 27 (2017) 170–174.
[32] C. Granzotto, K. Sutherland, Matrix assisted laser desorption ionization mass fingerprinting for identification of Acacia gum in microsamples from works of art, Anal. Chem. 89 (2017) 3059–3068.
[33] E. Angerson, Z. Bai, J. Dongarra, A. Greenbaum, A. McKenney, J.D. Croz, S. Hammarling, J. Demmel, C. Bischof, D. Sorensen, LAPACK: A Portable Linear Algebra Library for High-Performance Computers, Proceedings SUPERCOMPUTING '90, 1990, pp. 2–11.
[34] F. Pedregosa, G. Varoquaux, A. Gramfort, V. Michel, B. Thirion, O. Grisel, M. Blondel, P. Prettenhofer, W. Ron, V. Dubourg, J. Vanderplas, A. Passos, D. Cournapeau, M. Brucher, M. Perrot, D.É. Scikit-Learn, Machine learning in Python, J. Mach. Learn. Res. 12 (2011) 2825–2830.
[35] L. Van Der Maaten, Accelerating t-SNE using tree-based algorithms, J. Mach. Learn. Res. 15 (2014) 3221–3245.
[36] L. Van der Maaten, G. Hinton, Visualizing data using t-SNE, J. Mach. Learn. Res. 9 (2008) 2579–2605.
[37] A.K. Lakhera, V. Kumar, Monosaccharide composition of acidic gum exudates from Indian *Acacia tortilis* ssp. raddiana (Savi) Brenan, Int. J. Biol. Macromol. 94 (Part A) (2017) 45–50.
[38] P.R. Bhushette, U.S. Annapure, Comparative study of *Acacia nilotica* exudate gum and acacia gum, Int. J. Biol. Macromol. 102 (2017) 266–271.
[39] A. Grein, B.C. da Silva, C.F. Wendel, C.A. Tischer, M.R. Sierakowski, A.B.D. Moura, M. Iacomini, P.A.J. Gorin, F.F. Simas-Tosin, I.C. Riegel-Vidotti, Structural characterization and emulsifying properties of polysaccharides of *Acacia mearnsii* de Wild gum, Carbohydr. Polym. 92 (2013) 312–320.
[40] B. Domon, C. Costello, A systematic nomenclature for carbohydrate fragmentations in FAB-MS/MS spectra of glycoconjugates, Glycoconj. J. 5 (1988) 397–409.
[41] O.H.M. Idris, P.A. Williams, G.O. Phillips, Characterisation of gum from *Acacia senegal* trees of different age and location using multidetection gel permeation chromatography, Food Hydrocoll. 12 (1998) 379–388.
[42] M. Andres-Brull, I.G. Abdalla, J. Cirre, J. Edwards, M.E. Osman, G.O. Phillips, S. Al-Assaf, Studies on acacia gums: part VII effect of exudates form and tree age on the characteristics of *Acacia seyal* var. seyal and *Acacia seyal* var. fistula, Food Hydrocoll. 45 (2015) 279–285.
[43] E.A. Hassan, S. Al-Assaf, G.O. Phillips, P.A. Williams, Studies on Acacia gums: part III molecular weight characteristics of *Acacia seyal* var. seyal and *Acacia seyal* var fistula, Food Hydrocoll. 19 (2005) 669–677.
[44] N. Strudwick, Burial assemblages of dynasty 21–25: chronology, typology, developments, J. Egypt. Archaeol. 97 (2011) 294–297.
[45] O. Chiantore, C. Riedo, D. Scalarone, Gas chromatography–mass spectrometric analysis of products from on-line pyrolysis/silylation of plant gums used as binding media, Int. J. Mass Spectrom. 284 (2009) 35–41.
[46] C. Riedo, D. Scalarone, O. Chiantore, Advances in identification of plant gums in cultural heritage by thermally assisted hydrolysis and methylation, Anal. Bioanal. Chem. 396 (2010) 1559–1569.
[47] J.H. Ross, A Conspectus of African Acacia Species, (1979), p. 155.
[48] F. Casadio, H. Emily, K. Manchester, From the Molecular to the Spectacular: A Statue of Osiris through the Eyes of a Scientist, a Conservator, and a Curator, 31 Art Institute of Chicago Museum Studies, 2005, pp. 8–15.
[49] E.R. Russman, The statue of Amenemope-em-hat, Metrop. Mus. J. 8 (1973) 34–46.
[50] A. Langley, K. Sutherland, F. Casadio, S. Maccagnola, AIC Paintings Specialty Group Postprints, 28 (2015).